Irreversibilities in low-field magnetization of site-disordered $Ni_{75}Al_{25}$

Anita Semwal and S. N. Kaul*
School of Physics, University of Hyderabad, Central University P.O., Hyderabad-500 046, Andhra Pradesh, India
(Received 18 November 2002; revised manuscript received 21 February 2003; published 17 July 2003)

The results of extensive "zero-field-cooled" (M_{ZFC}) and "field-cooled" (M_{FC}) magnetization and hysteresis measurements performed in the magnetic field (H) and temperature (T) ranges 2.5 Oe$\leqslant H \leqslant$3 kOe (10 kOe) and $14K \leqslant T \leqslant 1.4T_C$ (Curie temperature) on $Ni_{75}Al_{25}$ samples with varying degree of site disorder and on samples with composition in the range $Ni_{74.31}Al_{24.69}$ to $Ni_{75.98}Al_{24.02}$ having the same degree of site disorder, are presented and discussed in the light of the existing theoretical models. The difference, $M_{irr}(T) = M_{FC}(T) - M_{ZFC}(T)$, is taken to be the direct measure of irreversibility in magnetization. As the temperature is lowered from $T \gg T_C$, M_{irr} as a function of temperature at a fixed H, (i) deviates from zero at a temperature T_{WI} (which marks the onset of weak irreversibility), (ii) goes through a *peak* at T_P (a *new feature*, to our knowledge not reported in the literature so far, observed in all the samples except for the quenched one), and (iii) exhibits a *steep* increase below T_{SI} (the temperature at which a crossover to strong irreversibility occurs). While the occurrence of a peak in $M_{irr}(T)$ has not been theoretically addressed yet, the observed variations of T_{WI} and T_{SI} with H as well as the observation that $T_{WI} \gg T_C$ and $T_{SI} \simeq T_C$ are in conflict with the predictions based on the mean-field vector-spin models. By establishing a clear link between the magnetic field variations of T_{WI}, T_P, and T_{SI} and the temperature dependences of H_C (coercive field), the present work asserts that the pinning of domain walls at the magnetic (exchange) inhomogeneities present in the samples under consideration is at the root of the observed irreversibilities in magnetization.

DOI: 10.1103/PhysRevB.68.024410 PACS number(s): 75.30.Kz, 75.60.Ej, 75.50.Cc

I. INTRODUCTION

Systems with widely different types of magnetic order such as spin glasses, ferromagnets, antiferromagnets, and ferrites exhibit irreversibilities in the low-field magnetization at temperatures below the ordering temperature regardless of whether they are crystalline or amorphous, metallic or insulating. A phenomenon so widespread has, however, received selective attention among magnetic materials: more in spin glasses and relatively less in ferromagnets/antiferromagnets. Thus, it is not surprising that more progress has been made in understanding this phenomenon in spin glasses than in other magnetic systems.

Mean-field (MF) vector spin models[1,2] predict *finite-temperature* phase transition in *zero* as well as *finite* magnetic fields for both Ising (spin dimensionality $n=1$) and Heisenberg ($n=3$) spin-glass (SG) systems. In an Ising SG system, this transition in the field-temperature (H-T) phase diagram occurs along the de Almeida–Thouless (AT) line[1]

$$\tau_f^3(h) = \{1-[T_f(H)/T_f(0)]\}^3 = (3/4)h^2 \tag{1}$$

[where the *reduced* field $h = g\mu_B H/k_B T_f(0)$ is *small* and $T_f(0)$ is the SG freezing temperature at $H=0$] and is signaled by an irreversibility in the magnetization. In an *isotropic* spin glass system composed of vector spins with n components, transitions in the H-T plane occur at *low* fields along two phase transition lines[2]: the Gabay-Toulouse (GT) line[2]

$$\tau_{GT}(h) = 1-[T_{GT}(H)/T_f(0)] = Ch^2 \tag{2}$$

with $C=(n^2+4n+2)/4(n+2)^2$, followed at lower temperatures by another line,[2]

$$\tau_{AT}^3(h) = \{1-[T_{AT}(H)/T_f(0)]\}^3 = C' h^2, \tag{3}$$

with $C'=(n+1)(n+2)/8$, which reduces to the AT form, [Eq. (1)], for $n=1$. The GT line marks the onset of weak irreversibility in the magnetization brought about by the freezing of spin degrees of freedom *transverse* to the field direction while the AT line signals a *crossover* from *weak* to *strong* irreversibility caused by the freezing of spin degrees of freedom *along* the field direction. In spin glass systems with random anisotropy (resulting from anisotropic Dzyaloshinsky-Moriya interactions), Kotliar and Sompolinsky[3] (KS) contended that random anisotropy significantly alters both the form and nature of the finite-field transition even when the anisotropy is so weak as to practically have no effect on the zero-field transition. The KS model[3] predicts that in the *strong anisotropy regime*, the transition is of the AT type, in that the transition line is described by Eq. (3) but with C' replaced by $C''=(n+2)/4n$, whereas in the *weak-anisotrtopy limit*, the transition is identical to the GT one, i.e., Eq. (2), but the zero-field transition temperature $T_f(0)$ shifts to lower temperatures by an amount[4] that depends on the magnitude of anisotropy. According to the KS model, the magnetic field should induce a crossover from the AT to GT irreversibility lines. A number of experiments have confirmed the existence[5–8] of GT and AT irreversibility lines in the H-T phase diagrams of several spin-glass systems and a field-induced AT→GT crossover[6–8] at a certain field-dependent temperature as the temperature is lowered, as predicted by the MF vector spin models.[1–4] However, such a behavior is not universal in the sense that, in some spin glasses, irreversibility lines do not obey Eq. (3). The deviations from the AT behavior have been understood in terms of a non-mean-field scaling theory.[9]

According to mean-field vector spin models,[2,10] in ferromagnets, the GT and AT lines are associated with the formation of the reentrant phase, which is essentially a canted ferromagnet with transverse spin-glass order and a longitudinal spontaneous magnetization M_S, and the external magnetic field (H) leaves the functional dependence of T_{AT} on h, i.e., Eq. (3), *unaltered* but *changes* the field dependence of T_{GT} from $T_{GT} \sim h^2$, i.e., Eq. (2), to[10]

$$\tau_{GT}(h) = 1 - [T_{GT}(H)/T_{GT}(0)] = (2^{3/2}C)h, \qquad (4)$$

where $T_{GT}(0) \equiv T_{GT}(H=0)$ is the GT transition temperature in the absence of H. Equation (4) is valid for $H \ll M_S$. An unambiguous correlation between the observed irreversibility lines in the H-T phase diagram of ferromagnets exhibiting a reentrant behavior at low temperatures with the GT and AT phase boundaries could not be established[10–12] so far.

Irreversibilities in the magnetization of reentrant ferromagnetic or antiferromagnetic systems have also found alternative interpretations[12–15] in terms of the non-mean-field models that include the phenomenological models, proposed independently by Coles *et al.*[16] and Kaul,[17] and invoke the mechanism of thermally activated depinning of domain walls. Unlike mean-field models, the models due to Coles *et al.*[16] and Kaul[17] assert that the irreversibility lines do not represent true thermodynamic phase transition lines (for details, see Refs. 12 and 18). However, even among the interpretations of such irreversibilities offered by various non-mean-field models, there is no general agreement.

Varied explanations for the phenomenon of irreversibility in magnetization in spin systems with long-range magnetic order calls for a deeper study of such systems than attempted hitherto. To this end, an extensive investigation of irreversibilities in the magnetization of weak itinerant-electron ferromagnets $Ni_{75\pm x}Al_{25\mp x}$ ($x=0,1$), "prepared" in different states of site disorder, has been undertaken. The rationale behind the choice of these samples is that they are devoid of the complications arising from the presence of a spin glass or a reentrant phase at low temperatures and permit determination of the role of site disorder, if any, in affecting irreversibilities in the magnetization.

II. EXPERIMENTAL DETAILS

Since details of the preparation and characterization of some of the samples are given elsewhere,[19,20] only the essential ones are briefly described here. Starting with the high-purity (99.999%) raw materials nickel and aluminum, polycrystalline alloys with a nominal composition $Ni_{75\pm x}Al_{25\mp x}$ ($x=0,1$) and a single crystal of nominal composition $Ni_{75}Al_{25}$ were prepared under a high-purity (99.999%) argon gas inert atmosphere by radio frequency induction and zone refining techniques, respectively. Spheres of 3-mm diameter (a cylinder with cylindrical axis parallel to the easy direction of magnetization, i.e., [111] direction) were spark cut from the polycrystalline rods (single crystal rod). One of the $Ni_{75}Al_{25}$ spheres was annealed at 520 °C for 16 days in a quartz tube evacuated to a pressure of 10^{-6} Torr and subsequently water quenched. A portion of the polycrystalline $Ni_{75}Al_{25}$ rod was melt quenched[20] onto a rotating copper wheel to form long thin ribbons of a width of 2 mm and a thickness of 30 μm. The samples of the alloy series $Ni_{75\pm x}Al_{25\mp x}$, in the "as-prepared" condition, are labeled as S_{74}, S_{75}, and S_{76}. The annealed, quenched, and *polycrystalline* samples, and the *single crystal* of nominal composition $Ni_{75}Al_{25}$, are henceforth referred to as S_1, S_2, and Z_{75}, respectively. The pieces remaining after spark cutting samples S_1, S_{74}, S_{75}, S_{76} and Z_{75} as well as ribbon pieces of the sample S_2 were analyzed for chemical composition using the x-ray fluorescence technique and inductively-coupled-plasma optical emission spectroscopy. The actual composition of these samples is given in Table I.

TABLE I. Nominal and actual composition, and Curie temperature of the samples under consideration.

Sample	Nominal composition		Actual composition		Curie temperature
	Ni (at %)	Al (at %)	Ni (at %)	Al (at %)	T_C (K)
S_1	75.00	25.00	75.08(17)	24.92(10)	56.377(5)
S_2	75.00	25.00	75.08(17)	24.92(10)	36.002(5)
S_{74}	74.00	26.00	74.31(17)	25.69(19)	47.60(5)
S_{75}	75.00	25.00	74.73(17)	25.27(19)	56.240(5)
S_{76}	76.00	24.00	75.98(9)	24.02(10)	76.298(5)
Z_{75}	75.00	25.00	74.33(16)	25.67(15)	41.00(10)

Extensive x-ray diffraction measurements, using CuK_α radiation, have been performed at room temperature on these samples over the angle, 2θ, in a range of $10° \lesssim 2\theta \lesssim 100°$ with a view to accurately determine[20] lattice parameters and the long-range atomic order parameter, which is a direct measure of the degree of site disorder present. The values of the Curie temperatures, T_C, for the samples in question (Table I) have been determined using an elaborate critical-point analysis[20] of the bulk magnetization and ac susceptibility data taken on them previously.

Each of the samples S_1, S_2, Z_{75}, S_{74}, S_{75}, and S_{76} was cooled down to 14 K in a zero external magnetic field from temperatures as high as $2T_C$ and, using the EG&G Princeton Applied Research 4500 Vibrating Sample Magnetometer, the zero-field-cooled magnetization (M_{ZFC}) was measured at constant (to within ± 5 mK) temperatures 0.5 K apart in the heating cycle from 14 K to $T \simeq T_C + 10$ K after a static magnetic field (H) of *fixed* magnitude in the range 2.5 Oe$\leqslant H \leqslant$1 kOe was applied. The samples were then cooled in the same field without changing the configuration and the static magnetization $[M_{FC}(T)]$ was measured at fixed (0.5 K) temperature steps in the cooling run [i.e., in the field-cooled (FC) mode]. Such magnetization curves at different but fixed values of the field, representative of the samples in question, are shown in Fig. 1.

Magnetic hysteresis loops have been recorded at fixed temperatures (stable to ± 10 mK) ranging from 14K to temperatures well above T_C in the field range -3 kOe$\lesssim H \lesssim$3 kOe (in some cases in the range -10 kOe$\lesssim H \lesssim$10 kOe as well) using the following modes of measurement. In the first mode of measurement [the so-called zero-

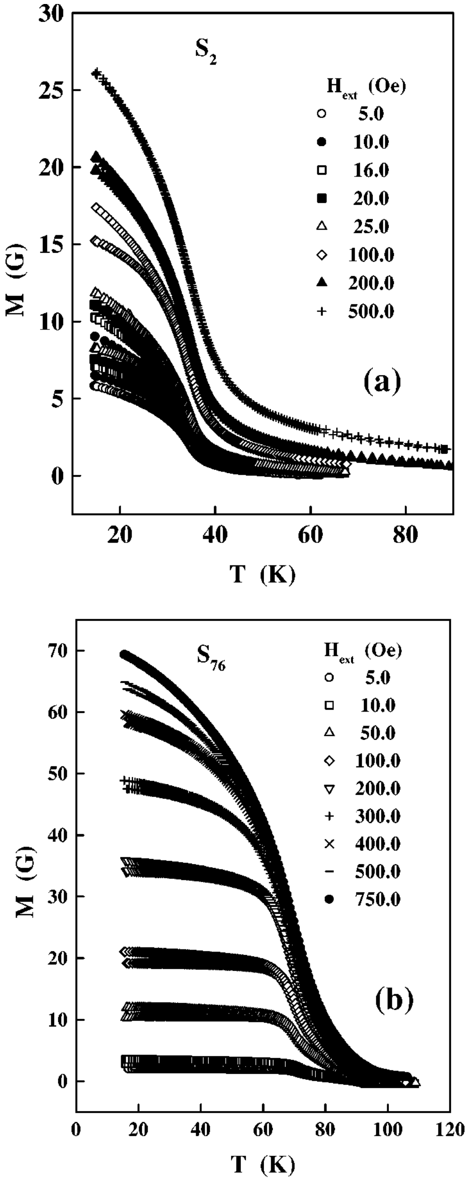

FIG. 1. Temperature variations of the ''zero-field-cooled'' (lower curves) and ''field-cooled'' (upper curves) magnetizations at different but fixed values of external magnetic field for samples (a) S_2 and (b) S_{76}.

field-cooled (ZFC) mode], the sample was cooled to the measuring temperature in zero-field from $T \simeq 2T_C$ before recording the M-H loops. In the second mode (the so-called field-history mode), the sample was cooled to the lowest measuring temperature ($\simeq 14$ K) in zero-field from $T \simeq 2T_C$ and the M-H hysteresis loops were recorded in the heating cycle after holding the sample temperature constant at different values in the range $14K \lesssim T \lesssim 1.5T_C$. In this mode, sample has the memory of field cycling it was subjected to at the previous value of temperature. Both types of measurements yield identical hysteresis loops (which are *symmetric* and *centered* at the origin $H=0$ and $M=0$) at a given temperature in the range covered in the present experiments for all the samples *except* for the quenched sample S_2 for $T > T_C$. To elucidate this point further, in sample S_2, the hysteresis loops are identical and centered (centred) at the origin in both the modes of measurement (only in the ZFC mode) for $T < T_C$ ($T > T_C$); in the case of the ''field-history'' mode, the center of the hysteresis loops shifts progressively to negative fields as the temperature is raised above T_C, as is evident from Fig. 2.

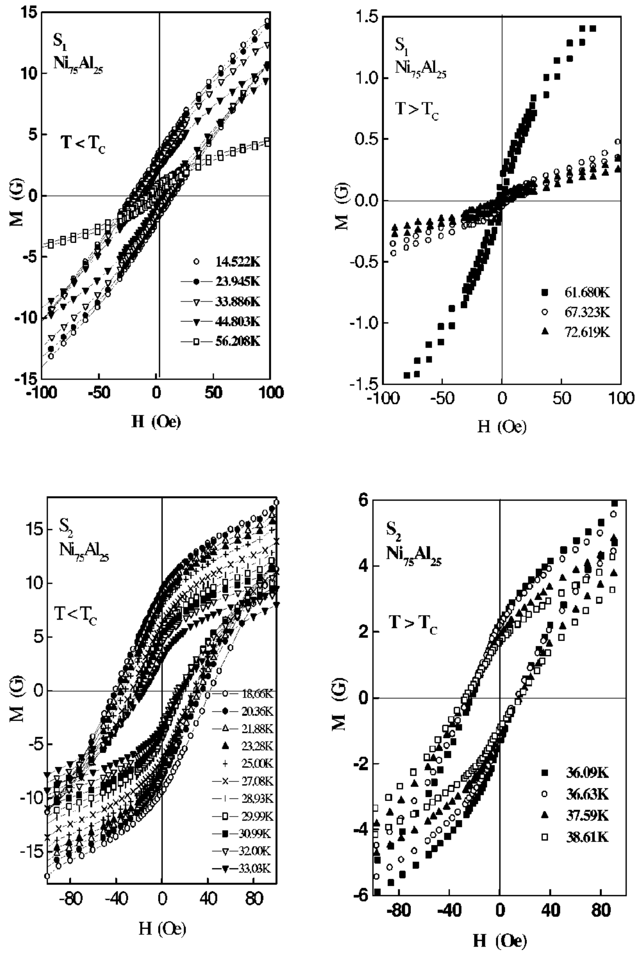

FIG. 2. M-H hysteresis loops at temperatures below and above Curie temperature for samples S_1 and S_2.

III. RESULTS

A. Magnetic irreversibility

From the data presented in Fig. 1, it is observed that the $M_{ZFC}(T)$ and $M_{FC}(T)$ curves do not fall on each other for temperatures below a certain characteristic temperature which depends on H. The difference between M_{FC} and M_{ZFC} at a given temperature and field is a *direct measure* of irreversibility in the magnetization $[M_{irr}(H,T)]$ at that temperature and field. The plots of $[M_{FC}(T) - M_{ZFC}(T)]$ versus temperature at different but fixed values of H are shown for samples S_2 and S_{76} in Fig. 3. The *representative* $M_{irr} = [M_{FC} - M_{ZFC}]$ curves (taken at fixed H) depicted in Fig. 3 present the following striking features. The difference $[M_{FC} - M_{ZFC}] = M_{irr}$ (i) deviates from zero below the temperature $T_{WI}(H) > T_C$ (the Curie temperature) which marks the onset of *weak irreversibility* (WI) in the magnetization,

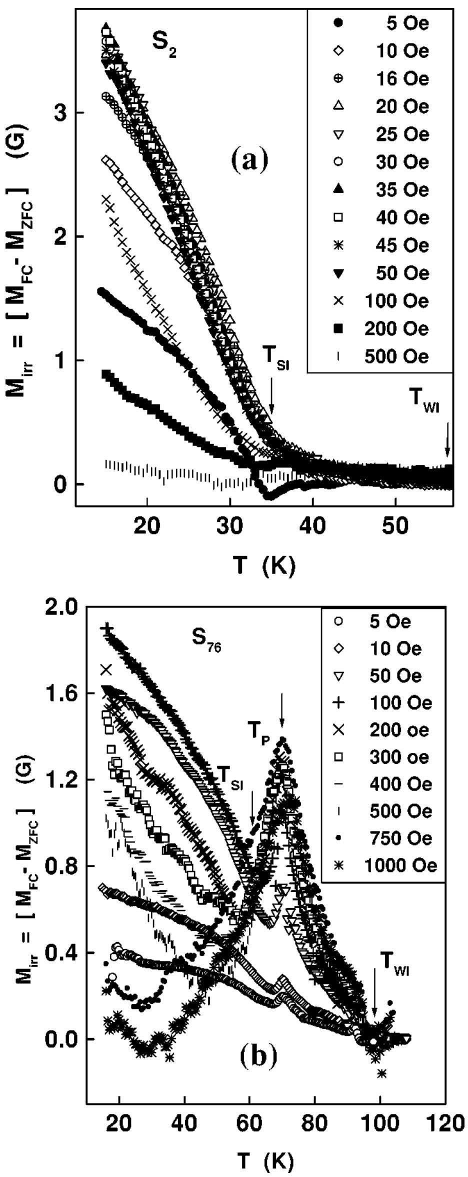

FIG. 3. The difference between field-cooled (M_{FC}) and zero-field-cooled (M_{ZFC}) magnetizations as a function of temperature at fixed values of external magnetic field for the samples (a) S_2 and (b) S_{76}.

(ii) goes through a peak (observed in all the samples except for the quenched sample S_2) at the temperature $T_P(H)$ ($\simeq T_C$), and (iii) increases steeply below the temperature $T_{SI}(H)(\lesssim T_C)$ which signals the onset of *strong irreversibility* (SI) in the magnetization. The irreversibility lines [loci of $T_{WI}(H)$, $T_P(H)$, and $T_{SI}(H)$ temperatures] in the *T-H* phase diagrams of the samples $S_1, Z_{75}, S_{74}, S_{75}$, and S_{76} follow, at low fields ($H \lesssim H^{**}$), the relations (Figs. 4–6)

$$\tau_{WI}(H) \equiv 1 - [T_{WI}(H)/T_{WI}(0)] = -H/H^*_{WI}, \qquad (5)$$

$$\tau_P(H) \equiv 1 - [T_P(H)/T_P(0)] = H/H^*_P, \qquad (6)$$

and

$$\tau_{SI}(H) \equiv 1 - [T_{SI}(H)/T_{SI}(0)] = H/H^*_{SI}, \qquad (7)$$

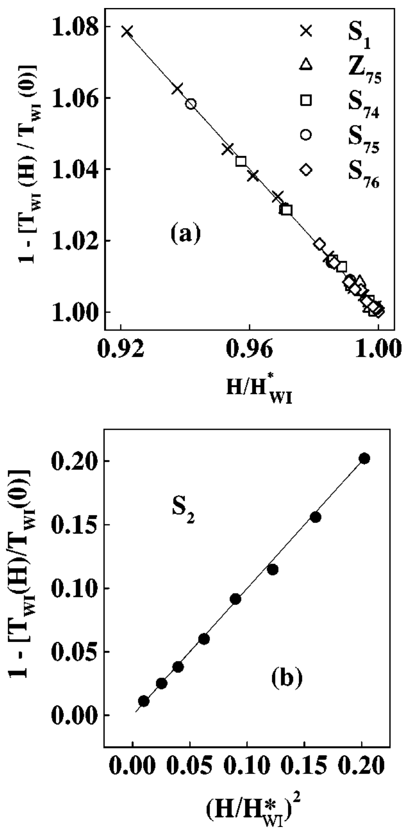

FIG. 4. Scaling of the reduced weak irreversibility temperature with the (a) reduced field for samples S_1, Z_{75}, S_{74}, S_{75}, and S_{76} and (b) reduced field squared for sample S_2.

By comparison, in the quenched sample (S_2), the relation $\tau_{SI}(H) \sim H$ [i.e., Eq. (7)], as in other cases, is *obeyed*, the $\tau_P - H$ irreversibility line does not exist, and the weak irreversibility line is described by the expression

$$\tau_{WI}(H) \equiv 1 - [T_{WI}(H)/T_{WI}(0)] = (H/H^*_{WI})^2 \qquad (8)$$

[which is at variance with Eq. (5), as is notable from the data presented in Fig. 4(b)]. In these expressions, the characteristic field H^* varies from sample to sample and hence depends on the degree of site disorder or chemical disorder present.

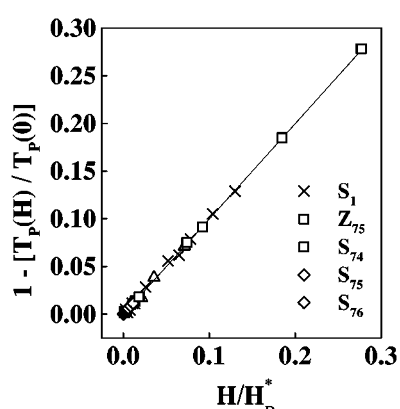

FIG. 5. Scaling of the reduced peak irreversibility temperature with the reduced field.

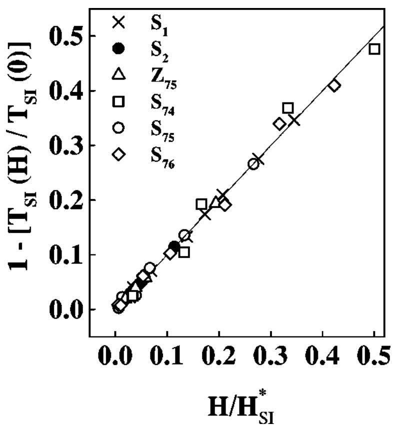

FIG. 6. Scaling of the reduced strong irreversibility temperature with the reduced field.

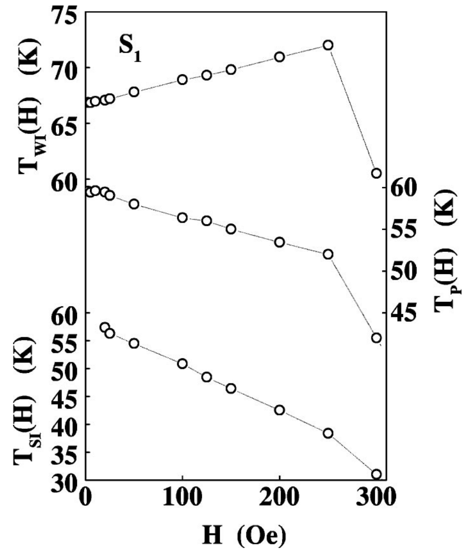

FIG. 7. Representative plots of the weak irreversibility, peak irreversibility and strong irreversibility temperatures T_{WI}, T_P and T_{SI} vs field.

The numerical values of the quantities $T_{WI}(0)$, H^*_{WI}, $T_P(0)$, H^*_P, $T_{SI}(0)$, H^*_{SI}, and H^{**} are listed in Table II.

Beyond a threshold field H_{cr} (whose value varies from sample to sample, as is evident from the magnitudes of H_{cr} displayed in Table II), the $M_{FC}(T)$ and $M_{ZFC}(T)$ curves coincide with one another down to the lowest measuring temperature, i.e., 14 K. This implies that H_{cr} is the field strength at and above which the irreversibilities cease to exist for $T \gtrsim 14K$. Representative $T_{WI}-H$, T_P-H and $T_{SI}-H$ plots, shown in Fig. 7 serve to highlight the finding that all the characteristic temperatures T_{WI}, T_P, and T_{SI} for irreversibility in magnetization suddenly drop even for fields well below H_{cr}. That the height of the peak in $M_{irr}(T)$, $m(H)$, initially *increases* with the field H, reaches a *maximum* m_{max} at a certain value of H (which is *sample-dependent*), and drops to zero at the critical field H_{cr}, is shown in Fig. 8. This figure also serves to demonstrate that the ratio m/m_{max}, when plotted against H/H_{cr} for all the samples, causes the $m(H)$ curves to fall onto one universal curve.

B. Magnetic hysteresis loops

Figure 2 demonstrates that, irrespective of temperature, the hysteresis loops are much broader (i.e., an order of magnitude higher H_C) in the case of the quenched sample S_2 than in other samples. The hysteresis loops for the samples in question in the ''field-history'' mode are depicted in Fig. 2 in a narrow field range of -100 Oe$\lesssim H \lesssim 100$ Oe because the coercive fields (H_C) are of the order of a few Oe. The variations of the remanent magnetization (M_r) and H_C with temperature for all the samples are shown in Figs. 9 and 10. Note that the H_C values at $T > T_C$ for the sample S_2 (solid triangles in Fig. 10) refer to the centers of the hysteresis loops depicted in Fig. 2. It is noticed from the data presented in these figures that (i) $M_r(T)$ almost mimics the temperature variation of the spontaneous magnetization $[M_S(T)]$ for $T \lesssim T_C$ but does not go to zero at T_C as $M_S(T)$ does; and (ii) $H_C(T)$, like $M_r(T)$, does not vanish at T_C but remains finite even for temperatures well above T_C.

IV. DISCUSSION

The mean-field vector-spin models, applicable to ferromagnets exhibiting a reentrant behavior at low temperatures, predict that at low fields $\tau_{WI}(H) \sim H$ [Eq. (4)], and $\tau_{SI}(H) \sim H^{2/3}$ [Eq. (3)]. The theoretically predicted field depen-

TABLE II. Fit parameters $T_{WI}(0)$, H^*_{WI}, $T_P(0)$, H^*_P and $T_{SI}(0)$, H^*_{SI} in Eqs. (5)–(8) and the corresponding values of H^{**} and H_{cr} for samples S_1, S_2, Z_{75}, S_{74}, S_{75}, and S_{76}.

Sample	Weak irreversibility			Peak			Strong irreversibility			
	$T_{WI}(0)$ (K)	H^*_{WI} (kOe)	H^{**}_{WI} (Oe)	$T_P(0)$ (K)	H^*_P (kOe)	H^{**}_P (Oe)	$T_{SI}(0)$ (K)	H^*_{SI} (kOe)	H^{**}_{SI} (Oe)	H_{cr} (Oe)
S_1	66.75(2)	3.20(3)	250	59.70(6)	1.92(3)	250	58.66(15)	0.725(11)	250	500
S_2	56.03(13)	0.100(1)	45	-	-	-	35.01(1)	0.874(4)	100	500
Z_{75}	68.92(8)	3.5(2)	100	49.68(1)	7.1(2)	100	49.76(2)	0.515(2)	100	-
S_{74}	70.67(3)	3.51(7)	150	61.11(5)	0.541(3)	150	51(1)	0.30(2)	150	600
S_{75}	68.09(2)	3.43(3)	200	63.45(22)	1.4(1)	100	49.77(28)	0.749(32)	200	800
S_{76}	94.89(3)	55(2)	1000	70.16(1)	8.7(1)	1000	68.62(52)	0.946(18)	500	3000

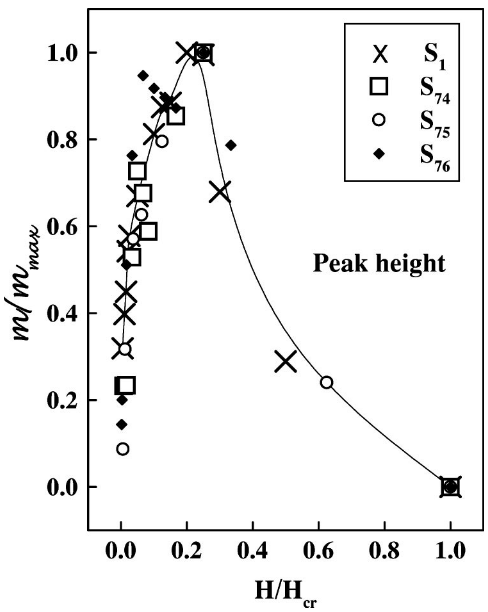

FIG. 8. Reduced peak height m/m_{max} vs the reduced field, H/H_{cr}.

dences do not conform to the observed ones as is evident from the following remarks. If τ_{WI} (τ_{SI}) is identified with τ_{GT} (τ_{AT}), according to the theoretical predictions, i.e., Eqs. (4) and (3), τ_{WI} and τ_{SI} should *increase* with magnetic field as H and $H^{2/3}$, respectively. However, in the samples S_1, Z_{75}, S_{74}, S_{75}, and S_{76}, τ_{WI}, instead of increasing, *decreases* linearly with H [Fig. 4(a)] as contrasted with the sample S_2 in which τ_{WI} *increases* with magnetic field not as H but as H^2 [Fig. 4(b)], while τ_{SI} does not increase as $H^{2/3}$ but increases *linearly* with H (Fig. 6) for all the samples. None of the existing theories predicts a peak in the magnetic irreversibility versus temperature (i.e., $[M_{FC}-M_{ZFC}]$ vs T) curves. Moreover, in sharp contrast with the theoretical prediction[16] that in ferromagnets with reentrant behavior at low temperatures, the Gabay-Toulouse irreversibility line lies *well below* the Curie temperature T_C and is followed at lower temperatures by the Almeida-Thouless instability line, weak

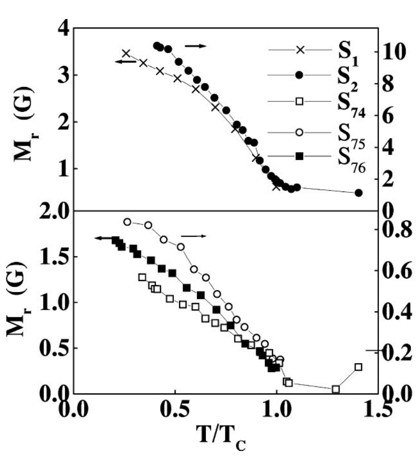

FIG. 9. Remanent magnetization as a function of reduced temperature.

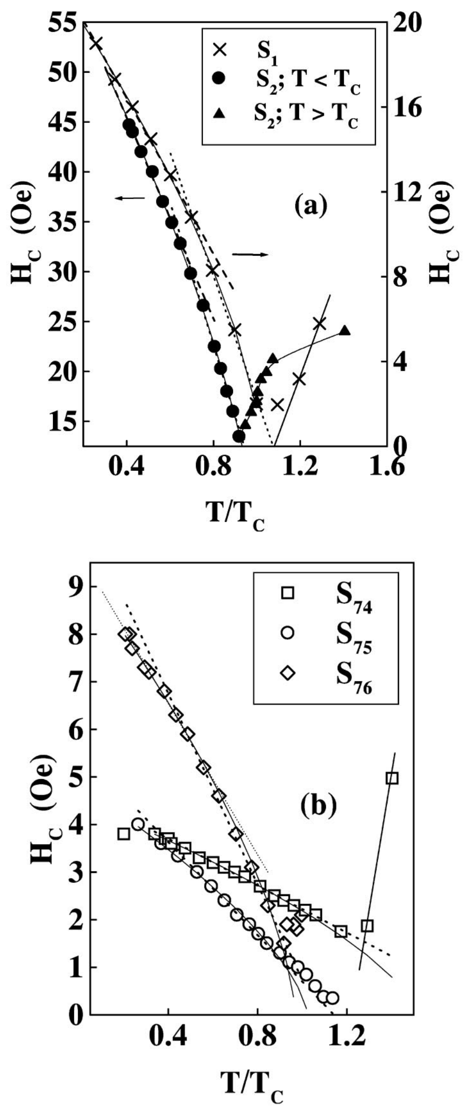

FIG. 10. Coercive field as a function of reduced temperature for samples (a) S_1 and S_2 and (b) S_{74}, S_{75}, and S_{76}.

irreversibility line $T_{WI}(H)$ lies *well above* T_C while the strong irreversibility line $T_{SI}(H)$ is located *close* to T_C for all the samples under consideration. Such a wide disparity between the theoretical predictions and experimental observations may not be surprising in view of the fact that the presently investigated systems do not exhibit a reentrant or spin glass behavior.

In conventional ferromagnets, irreversibility in the magnetization at low fields, and temperatures well below T_C, is normally attributed to the progressive stiffening of domain walls (alternatively, to the increase in magnetic viscosity) as the temperature is lowered through T_C to low temperatures. By contrast, in the samples of the $Ni_{75}Al_{25}$ alloy that vary either in the degree of site disorder or slightly in composition, irreversibility in the magnetization at low fields is first observed at temperatures well above T_C. The occurrence of irreversibility at $T>T_C$ suggests that the above mechanism may not be relevant to the present case. Nevertheless, an

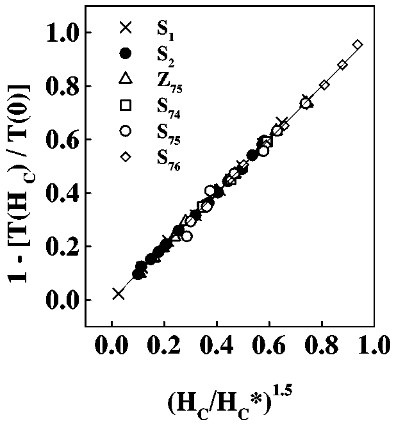

FIG. 11. Reduced temperature vs reduced coercive field, $(H_C/H_C^*)^{1.5}$.

attempt is made to ascertain if anisotropy and/or inhomogeneities and/or pinning effects are at the root of the observed irreversibility. To this end, an extensive study of magnetic hysteresis in the samples under consideration was undertaken, as detailed in Sec. II.

In order to facilitate a comparison between $H_C(T)$ and the characteristic irreversibility temperatures $T_{WI}(H)$, $T_P(H)$ and $T_{SI}(H)$, $H_C(T)$ data are converted into $T(H_C)$ data such that $T(H_C)$ denotes the temperature corresponding to a given value of H_C. Figure 11 clearly demonstrates that the $T(H_C)$ data, so obtained, follow the relation

$$\tau(H_C)=1-[T(H_C)/T(0)]=(H/H_C^*)^{1.5} \qquad (9)$$

for $T\lesssim T_C$, or equivalently, for $H_C\gtrsim H_C^{**}$, regardless of the degree of site disorder present or the alloy (Ni_xAl_{100-x}) composition in the range $74.31\lesssim x\lesssim 75.98$ at %. The values for $T(0)$, H_C^*, and H_C^{**} are listed in Table III. The best least-squares fits based on Eq. (9) are depicted in Fig. 10 by the continuous curves. A comparison of Eq. (9) with Eqs. (5)–(8) reveals that the field dependence of τ does not conform to the variations of τ_{WI}, τ_P, and τ_{SI} with H. At the first sight, this disparity may be taken to indicate that different mechanisms are responsible for the irreversibility in the magnetization and coercivity. However, close scrutiny reveals that within the temperature range wherein the values of $\tau_P(H)$ and $\tau_{SI}(H)$ for a given sample fall, H_C decreases *linearly* with increasing temperature (dotted straight lines in

TABLE III. $T(0)$, H_C^* and H_C^{**} values for the samples S_1, S_2, S_{74}, S_{75}, and S_{76}. The typical errors in the values of H_C^{**} is ± 0.5 Oe.

Sample	$T(0)$ (K)	H_C^* (Oe)	H_C^{**} (Oe)
S_1	59.19(38)	22.76(14)	2
S_2	36.77(12)	63.42(20)	14.5
S_{74}	73.26(65)	4.50(3)	2.3
S_{75}	56.31(29)	4.89(3)	1.1
S_{76}	73.31(47)	9.40(5)	1.5

TABLE IV. T range, $T(0)$, H_0 and H_C^+ values for samples S_1, S_2, S_{74}, S_{75}, and S_{76}. The typical errors in the values of H_C^+ is ± 0.5 Oe.

Sample	Temperature range (K)	$T(0)$ (K)	H_0 (Oe)	H_C^+ (Oe)	$T_P(0)$ $[T_{SI}(0)]$ (K)
S_1	44.8-56.2	59.64(5)	0.0	35.57	59.70(6)
S_2	28.93-33.03	39.25(5)	0.0	85.76	[35.01(10)]
S_{74}	26.10-46.70	61.13(6)	1.59	3.06	61.11(5)
S_{75}	20.68-50.67	63.38(7)	0.32	4.9	63.45(22)
S_{76}	33.10-70.00	70.00(8)	1.60	9.15	70.16(10)

Fig. 10). In view of this observation, the $H_C(T)$ data in the specified temperature ranges (Table IV) have been recast in the form $\tau(H_C)$ and least-squares fitted to the expression

$$\tau(H_C)=1-[T(H_C)/T(0)]=(H_C-H_0)/H_C^+. \qquad (10)$$

The outcome of this exercise, shown in Fig. 12, asserts that for all the samples under consideration, τ indeed has the *same* dependence on field as $\tau_P(H)$ and $\tau_{SI}(H)$ have. Moreover, from the values of the parameters $T(0)$, H_0 and H_C^+, listed in Table IV, a perfect agreement between the values of $T(0)$ and $T_P(0)[T_{SI}(0)]$ for the samples S_1, S_{74}, S_{75}, and S_{76} (sample S_2) is clearly noticed. As far as the weak irreversibility is concerned, the *linear* increase in H_C with temperature for $T>T_C$ (indicated by the scanty data in Fig. 10) in the case of samples S_1, S_{74}, S_{75}, and S_{76} augurs well with the *linear* decline in τ_{WI} with increasing H [Eq. (5)], observed in these samples at $T>T_C$ [Fig. 4(a)]. The above agreement suggests that the same underlying mechanism may be responsible for both $\tau(H_C)$ and $\tau_P(H)$ or $\tau_{SI}(H)$ [$\tau(H_C)$ and $\tau_{WI}(H)$] for $T\lesssim T_C$ $(T>T_C)$.

Now that there are strong indications that H_C and the irreversibilities in the magnetization may have a common origin to start with, we focus our attention on the temperature dependence of H_C (Fig. 10). The $H_C(T)$ data shown in Fig. 10 demonstrate that H_C decreases linearly with increasing temperature up to a temperature T^* (which varies from $\simeq 0.6T_C$ to T_C depending on the sample), and for $T>T^*$ the

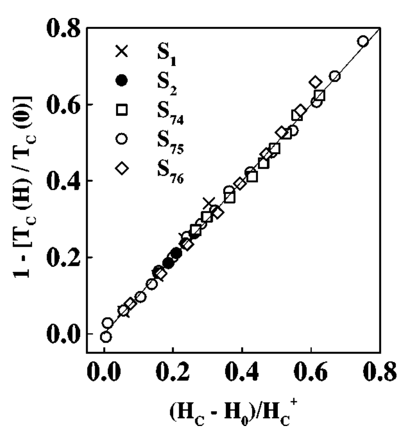

FIG. 12. Reduced temperature vs reduced coercive field, $(H_C-H_0)/H_C^+$.

rate of decline in H_C is faster. The theory due to Guant[21] considers domain-wall pinning by sample inhomogeneities as the main mechanism for remanence and coercivity in real magnetic materials. In the conventional terminology, *pins* are impediments to domain-wall motion that locally decrease the wall energy. According to this theory, the temperature dependence of the coercive field is given by the expression

$$H_C(T)=H_C(0)[1-(25k_B/31\gamma b^2)T], \tag{11}$$

where γ is the domain-wall energy per unit area and $4b$ is the range of interaction between the domain wall and the pin. For weak pinning, the domain wall breaks away simultaneously from many pins and the statistical fluctuations of pin density essentially determine the value of H_C at $T=0K$, i.e., $H_C(0)$. The linear temperature dependence of H_C predicted by Eq. (11), when the product γb^2 remains *constant*, conforms well with the observed $H_C(T)$ for $T<T^*$ (Fig. 10). The departure from the linear temperature dependence of H_C for $T>T^*$ (Fig. 10) thus basically reflects the fact that the product γb^2 is no longer independent of temperature. For a 180° domain wall in a ferromagnet with uniaxial anisotropy, domain-wall energy[21] is $\gamma=4\sqrt{(AK_1)}$ and the wall width[21] is $4b=4\sqrt{(A/K_1)}$, where A is the exchange energy per unit length and K_1 is the leading uniaxial anisotropy constant. Since both A and K_1 are temperature dependent, the product γb^2 need not be independent of temperature in the entire temperature range $0\lesssim T\lesssim T_C$.

So far as the presently investigated samples are concerned, site disorder and/or chemical disorder give rise to *local* compositional fluctuations (*local* atomic density fluctuations) which, according to the phenomenological model proposed earlier by Coles *et al.*[16] (Kaul[17]) result in the formation of *finite* ferromagnetic (FM) spin clusters that coexist with the *infinite* three-dimensional FM matrix at $T<T_C$. In the regions that surround the finite FM clusters, the exchange coupling between spins of clusters and the matrix is *weak* (because of quenched random-exchange disorder) and such regions act as pinning centers for the domain walls of the infinite FM matrix as they reduce the domain wall energy locally. Now that statistical fluctuations of the pin density, caused by site and/or chemical disorder, at the absolute zero of temperature essentially determine the value of $H_C(0)$, $H_C(0)$ varies from sample to sample.

The occurrence of strong and peak irreversibility in magnetization for temperatures in the immediate vicinity of T_C as well as of weak irreversibility in the magnetization at $T\gg T_C$ can be *qualitatively* understood in terms of the models due to Coles *et al.*[16] and Kaul[17] as follows. According to these models, the infinite FM network *disorders* at T_C while the finite FM spin clusters, by virtue of substantially higher *local* ordering temperatures, disorder at temperatures well above T_C. Thus, for $T>T_C$, finite FM spin clusters coexist with a paramagnetic matrix. Finite remanent magnetization (Fig. 9) and coercivity (Fig. 10) even at temperatures well above T_C in the present case strongly suggests the existence of a *trace* minority ferromagnetic Ni-rich phase (which escaped detection in the x-ray diffraction experiments) whose Curie temperature is much higher than that of the majority FM (Ni-poor) phase. As the temperature is raised through T_C, the domain structure of the majority phase disappears as $T\to T_C$ but that of the minority phase remains still in tact. Normally, the strong irreversibility would have paved the way for the weak irreversibility as $T\to T_C$ had only the majority phase been present. However, in the samples under consideration, the finite FM spin clusters belonging to the majority phase act as pinning centers for the domain walls of the minority phase at temperatures close to, and above, T_C. Consequently, the weak irreversibility in the magnetization of the main FM phase competes with the strong irreversibility in the magnetization of the minor phase FM phase to give rise to the peak in M_{irr} versus temperature curves [Fig. 3(b)] at different but fixed fields for temperatures close to T_C (the weak irreversibility in the magnetization of the major FM phase is completely masked in the process) whereas the weak irreversibility in the magnetization observed at $T\gg T_C$ actually corresponds to the minor FM phase. Moreover, the peak height increases with magnetic field up to a field $H\simeq 0.25H_{cr}$ (Fig. 8), because the domain walls encounter an increased number of pinning centers (finite FM clusters) as they traverse larger regions of a given sample under the influence of the magnetic field. As the field is increased beyond this threshold value, pinning becomes less and less effective, with the result that the peak height is progressively suppressed. Absence of the peak in $M_{irr}(T)$ particularly in the quenched sample [Fig. 3(d)] basically indicates that quenching does not favor the nucleation of the minor FM phase but instead leads to a fine dispersion of a large number of small-sized finite FM spin clusters (for details, see Ref. 17) in the infinite FM matrix such that the finite clusters do not (do) differ significantly in composition (atomic density) from the infinite matrix. Due to *high cluster density*, pinning of domain walls is stronger in this sample than in other samples for $T\lesssim T_C$ and even at temperatures well above T_C, strong competing interactions operate between the finite FM spin clusters. This explains the much stronger irreversibility (Fig. 3) and substantially larger magnitudes of M_r and H_C (Figs. 9 and 10), for $T\lesssim T_C$, on the one hand, and the field dependence of τ_{WI} [Fig. 4(b) and Eq. (8)] as well as the *field-history-dependent* shift in the center of the *M*-*H* hysteresis loops for $T>T_C$, *characteristic* of spin glasses or cluster spin glasses [cf. Eq. (2)], on the other hand, in the quenched sample S_2 as compared to the other samples.

V. CONCLUSION

The ''zero-field-cooled'' magnetization (M_{ZFC}) and 'field-cooled' magnetization (M_{FC}) have been measured at different but fixed values of magnetic field from 14 K to temperatures well above the Curie temperature on samples of composition $Ni_{75}Al_{25}$ with varying degrees of site disorder (S_1, S_2, and Z_{75}) and on samples of varied composition in the range $Ni_{74.31}Al_{25.69}$ to $Ni_{75.98}Al_{24.02}$ (S_{74}, S_{75}, and S_{76}), but with a *fixed* degree of site disorder. An elaborate analysis of such data permits an accurate determination of the weak, peak (not observed in sample 2) and strong irreversibility lines in the *T*-*H* phase diagram of the samples in question. The field dependences of the weak (Gabay-Toulouse) and strong (Almeida-Thouless) irreversibility temperatures predicted by the mean-field vector spin models for isotropic ferromagnets do not conform to those observed in the present case. A detailed comparison between the magnetic field variations of the temperatures T_{WI}, T_P, and T_{SI}, characterizing the weak, peak, and strong irreversibilities in the magnetization, and the temperature dependences of the coercive field reveal that coercivity and the irreversibilities in the magnetization have a common origin in the pinning of domain walls to the regions of *weak* exchange coupling. These regions are brought about by the site and/or compositional disorder present in the alloy samples under consideration.

*Author to whom all correspondence should be addressed. Email address: kaulsp@uohyd.ernet.in

[1] J.R.L. de Almeida and D.J. Thoules, J. Phys. A **11**, 983 (1978).
[2] M. Gabay and G. Toulouse, Phys. Rev. Lett. **47**, 201 (1981).
[3] G. Kotliar and H. Sompolinsky, Phys. Rev. Lett. **53**, 1751 (1984).
[4] K.H. Fischer, Z. Phys. B: Condens. Matter **60**, 151 (1985).
[5] R.V. Chamberlin, M. Hardiman, L.A. Turkevich, and R. Orbach, Phys. Rev. B **25**, 6720 (1982); P. Monod and H. Bouchiat, J. Phys. (France) Lett. **43**, L145 (1982); J.L. Tholence and M.B. Solomon, J. Magn. Magn. Mater. **31-34**, 1340 (1983).
[6] N. de Courtenay, A. Fert, and I.A. Campbell, Phys. Rev. B **30**, 6791 (1984).
[7] G.G. Kenning, D. Chu, and R. Orbach, Phys. Rev. Lett. **66**, 2923 (1991).
[8] F. Bernardot and C. Rigaux, Phys. Rev. B **56**, 2328 (1997).
[9] A.P. Malozenoff, S.E. Barnes, and B. Barbara, Phys. Rev. Lett. **51**, 1704 (1983).
[10] S.M. Dubiel, K.H. Fischer, Ch. Saver, and W. Zinn, Phys. Rev. B **36**, 360 (1987).
[11] H. Kunkel, R.M. Roshko, W. Ruan, and G. Williams, J. Appl. Phys. **69**, 5060 (1991).
[12] S.N. Kaul and S. Srinath, J. Phys.: Condens. Matter **10**, 11 067 (1998).
[13] D.A. Read, T. Moyo, and G.C. Hallam, J. Magn. Magn. Mater. **54-57**, 309 (1986).
[14] D.G. Rancourt, S. Chehab, and G. Lamarche, J. Magn. Magn. Mater. **78**, 129 (1989); D.G. Rancourt, *ibid.* **78**, 153 (1989).
[15] P.A. Joy, P.S. Anil Kumar, and S.K. Date, J. Phys.: Condens. Matter **10**, 11 049 (1998).
[16] B.R. Coles, B.V.B. Sarkissian, and R.H. Taylor, Philos. Mag. B **37**, 489 (1978).
[17] S.N. Kaul, Solid State Commun. **36**, 279 (1980); IEEE Trans. Magn. **20**, 1290 (1984); J. Magn. Magn. Mater. **53**, 5 (1985); J. Phys.: Condens. Matter **3**, 4027 (1991); S.N. Kaul and P.D. Babu, *ibid.* **10**, 1563 (1998).
[18] S.N. Kaul, Met., Mater. Processes **7**, 29 (1995).
[19] Anita Semwal and S.N. Kaul, Phys. Rev. B **64**, 014417 (2001); **60**, 12 789 (1999).
[20] Anita Semwal and S.N. Kaul, J. Phys.: Condens. Matter **14**, 5829 (2002).
[21] P. Gaunt, Can. J. Phys. **65**, 1194 (1987).